Atmospheric Environment 308 (2023) 119883

Contents lists available at ScienceDirect

Atmospheric Environment

journal homepage: www.elsevier.com/locate/atmosenv

Personal measurements and sampling of particulate matter in a subway – Identification of hot-spots, spatio-temporal variability and sources of pollutants

Jan Bendl [a,d,*], Carsten Neukirchen [a,c], Ajit Mudan [a], Sara Padoan [a,b], Ralf Zimmermann [b,c], Thomas Adam [a,b]

[a] University of the Bundeswehr Munich, Faculty for Mechanical Engineering, Institute of Chemical and Environmental Engineering, Werner-Heisenberg-Weg 39, 85577, Neubiberg, Germany
[b] Joint Mass Spectrometry Center (JMSC) at Comprehensive Molecular Analytics (CMA), Helmholtz Zentrum München, Ingolstädter Landstr. 1, 85764, Neuherberg, Germany
[c] Joint Mass Spectrometry Center (JMSC) at Chair of Analytical Chemistry, Institute of Chemistry, University of Rostock, Albert-Einstein-Strasse 27, 18059, Rostock, Germany
[d] Institute for Environmental Studies, Faculty of Science, Charles University, Benátská 2, 128 01, Prague 2, Czech Republic

HIGHLIGHTS

- Higher spatial than temporal variability of PM in the Munich subway system was observed.
- Significant differences in PM concentrations between platforms were found, with train frequency being a key factor.
- Iron oxide particles as products of rails and wheels abrasion dominated PM mass.
- Mobile measurements of subway systems effectively identify hot-spots and air quality.
- With the proposed methodology, subway systems can be comparably mapped for site-specific PM reduction measures.

GRAPHICAL ABSTRACT

ARTICLE INFO

Keywords:
Metro
Public transport
Indoor air quality
Personal exposure
Particulate matter
Elemental composition

ABSTRACT

A mobile measurement system for complex characterization of particulate matter (PM) was developed together with the proposed methodology and applied in the subway system of Munich, Germany. The main objectives were to observe the spatio-temporal variability of PM, personal exposure, identify hot-spots and pollution sources. Particle mass (PM_x) and number (PNC) concentrations, and equivalent black carbon (eBC) were measured at 0.1–1 Hz. On the *U5* subway line, PM_{10}, $PM_{2.5}$ and PM_1 concentrations at platforms ranged from 59 to 220, 27–80, and 9–21 μg m^{-3}, respectively. During rides towards downtown, average PM_{10}, $PM_{2.5}$ and PM_1 levels gradually increased from 8 to 220, 2 to 71 and 2–20 μg m^{-3}, respectively, with a similar dynamic of decrease on the return journey. Spatial variability of PM was generally more important than temporal, and

Abbreviations: PM, Particulate matter.

* Corresponding author. University of the Bundeswehr Munich, Faculty for Mechanical Engineering, Institute of Chemical and Environmental Engineering, Werner-Heisenberg-Weg 39, 85577, Neubiberg, Germany.
E-mail address: jan.bendl@unibw.de (J. Bendl).

https://doi.org/10.1016/j.atmosenv.2023.119883
Received 25 February 2023; Received in revised form 18 May 2023; Accepted 31 May 2023
Available online 1 June 2023

significant differences were observed between platforms. During the rides, air exchange between train and tunnel was high in both air-conditioned and old passively ventilated trains. Peak PM concentrations on platforms were associated with arriving/departing trains. Subway PNC were not significantly elevated, but a few cases of intake of traffic-related particles from outside were observed, otherwise air exchange was considered low. Generally, most of the aerosol mass was composed of iron corrosion products from rails and wheels (Fe up to 66 μg m^{-3} in $PM_{2.5}$). The effective density of $PM_{2.5}$ was 2.1 g cm^{-3}. Particles were classified as 75.4% iron oxides, 5.35% metallic Fe, 1.23% aluminosilicates and 17% carbon and oxygen rich particles. The iron oxide particles consisted predominantly of Fe (63.4 ± 8.7 wt%) and O (36.2 ± 8.2 wt%). To effectively monitor subway PM and reduce overall PM exposure, we propose to identify hot-spots using our methodology and focus on improving their ventilation, as well as installing filters in air-conditioned wagons.

1. Introduction

People in urban areas around the world spend a considerable amount of time commuting and often choose subway as the most sustainable and time-efficient environmentally friendly transport mode. However, personal exposure to harmful compounds within the transport microenvironment can pose a health risk (Cepeda et al., 2017). Even low concentrations of pollutants, such as ultrafine particles (UFP), can cause long-term adverse health effects (Schraufnagel, 2020). In general, the health effects of PM exposure ranging from respiratory diseases to cancer, result in significant impairment of quality of life, premature deaths and non-negligible economic impacts (World Health Organization, 2021). Minimizing exposure to PM in public transport is, therefore, necessary and in line with the objective of the United Nation's Sustainable Development Goal #11 (Huck, 2022) and the Guidelines for Developing and Implementing a Sustainable Urban Mobility Plan (Rupprecht Consult, 2019).

Subway stations and tunnels are a specific micro-environment dominated by non-exhaust emissions (NEE) from electric trains in relatively closed space. NEE are not yet regulated and systematically monitored like vehicle exhaust emissions. Nevertheless, PM_{10} and $PM_{2.5}$ concentrations in subways have been often found to exceed WHO ambient air quality guidelines (Xu and Hao, 2017; Chang et al., 2021). The negative health effects of subway PM have been proven in various studies. These include DNA damage caused most likely by the redox-active surfaces of metal-rich particles leading to oxidative stress (Karlsson et al., 2006, 2008), as well as inflammatory, toxicity and transient biological effects (Bachoual et al., 2007). Recent research has also revealed cancer risks associated with exposure to subway PM (Roy et al., 2022). However, not all mechanisms are fully understood yet.

The main sources of subway PM described in literature are abrasion from brakes (steel alloys containing chromium and nickel), rails and wheels (mostly iron) as well as rail catenary and pantographs (copper) with iron being dominant in $PM_{2.5}$ (Minguillón et al., 2018). Due to subway systems being enclosed environments, the effects of ventilation on air quality have been observed as well as other phenomena such as piston effects of trains, which resuspend settled dust (Martins et al., 2016; Cartenì et al., 2020).

Various studies focusing on personal exposure in the subway have been conducted (Querol et al., 2012; Yang et al., 2015; Xu et al., 2016; Shakya et al., 2020; Targino et al., 2021), however, the aim of this study is to present the most comprehensive approach to characterize subway PM exclusively using a custom-built mobile measurement system (followed by laboratory analysis). One of the aims was to propose a methodology to effectively identify hot-spots, measure the spatial and temporal dynamics of the aerosol, provide an indoor/outdoor PM comparison with respect to size distribution, elemental composition and morphology of the particles. In addition, personal exposure during typical rides and specific questions such as differences between old and new trains have been addressed.

Measurements were conducted in the Munich subway system, where there has been no published study to date. In our pilot study, on-line PM measurements were focused on PM_1, $PM_{2.5}$, PM_{10}, particle number concentration (PNC), equivalent black carbon (eBC) and lung deposited surface area (LDSA), which is a relatively new health-relevant metric combining alveolar deposition efficiency of particles with their surface area (Salo et al., 2021). Filter sampling for metal contents of PM analyzed by inductively coupled plasma mass spectrometry (ICP-MS) was performed either stationary at selected platforms or during typical journeys to assess citizen exposure. The morphology and elemental composition of individual particles were analyzed using scanning electron microscopy with energy dispersive X-ray spectroscopy (SEM-EDX).

2. Materials and methods

2.1. Study area

Mobile measurements were conducted in the area of Munich with 1.5 mio. inhabitants and an area of 311 km^2. Its subway system called *U-Bahn* consists of 8 lines (*U1-U8*), the first of which was completed in 1971. The total length of the rail network is about 95 km with 100 station platforms, tunnels with a maximum depth of 25 m and around 530 trains. In 2019, 429 million passengers used the subway for transportation, however, the numbers decreased due to the Covid-19 pandemic in 2020 (251 mio.) and 2021 (254 mio.; https://www.mvg.de/). Normally, the frequency of trains is 10 min, which shortens to 5 min during rush hours (7-9 am and 3-7 pm) and extends up to 30 min at the beginning (4 a.m.) and end (2 a.m.) of the service. Currently, three train types (A, B, C) with usually 6 cars are present, while only trains A (built 1967-1983) and C (build 2000 and later) were investigated. The "old" trains (A) have no ventilation system except for windows and the interior is separated into individual wagons while "new" trains (C) have ventilation, permanently closed windows and the interiors of three wagons are connected into one large volume. Focus of this study was on the line *U5* (Fig. S3 in SI), where "new" and "old" trains are randomly in operation. Trains are powered by a 750 V third rail made of low carbon steel (in the locations sampled) or aluminium. Outside of operating hours, the Munich Transport Service (MVG) occasionally uses a *Speno* train for grinding the rails and a special vacuum locomotive (VakTrak, New International Railways & SOCOFER) to clean the tracks from trash and sedimented particles using a blower and filtration system (*https://www.u-bahn-muenchen.de/*).

In Munich, the regional overground trains *S-Bahn* (*S1-S8*) often run in tunnels that are separated from the *U-Bahn* system with few exceptions. *S-Bahn* trains are ventilated with the possibility of opening the windows. The *S7* line was partially investigated in this study.

Hauptbahnhof (Munich Central Station) and *Ostbahnhof* are transfer stations to normal long-distance and regional trains.

Table 1 lists all stations included in this study along with abbreviations indicating *U-Bahn* (*U*), *S-Bahn* (*S*), or *railway* (*R*) stations. For example, the abbreviation *CS-R* stands for Munich central railway station and *CS-S* for Munich central station of *S-Bahn* trains. As there are two *U-Bahn* station platforms at the *Munich central station*, they are additionally numbered with the higher number indicating the deeper station (e.g. *CS-U2*). *NS-U/S* indicates the station *Neuperlach Süd* with a shared platform for *U-Bahn* and *S-Bahn*. The highlighted public transport map is in SI (Fig. S3) and all routes are shown in detail in Tables S2–S5.

2.2. Measurement strategy (proposed methodology)

The starting point of all personal measurements was at the Bundeswehr University Munich (GPS: 48°04′54.5″N 11°38′20.1″E) 1 km away from the terminal station *Neuperlach Süd* (*NS-U/S*, line *U5*), which is exceptionally above-ground. The ambient air quality station for reference measurements (section 2.6.) was located on the university campus.

The strategy of measurements and sampling is schematically reported in Fig. 1. As a first step, reference measurements in the surrounding area and different scouting rides within the subway were performed to identify hot-spots and to select typical routes for repetitions at different times of the day for the spatio-temporal variability of PM. Finally, stationary measurements were conducted with the mobile system at the center of the selected platforms to obtain information on the effects of arriving trains on the variability of PM. Therefore, the study was divided into the following experiments:

1) Mobile measurements of PM, PNC, and personal sampling for metals analysis (ICP-MS) on the university campus and surrounding urban micro-environments for reference (map of route in SI Fig. S2). A 1-h typical walking route **A** (Tables 2 and 3) was repeated 6 times and the new customized measurement system was tested
2) Scouting subway rides for PM, PNC observation, and identification of hot-spots (randomly selected routes **B, C, D, E**)
3) Repetition of the same ~1h long subway routes in the morning, noon and afternoon (selected based on previous results) to estimate daily variability (route **F**)
4) Stationary measurements and sampling (~3 h) at a platform identified as a hot-spot and considered to be a representative busy transfer station in the Munich city center for detailed characterization of particles using SEM/EDX and ICP/MS (**G**: platform *U5/U4* of Munich main train station *Hauptbahnhof CS-U1*). The dynamics of the particle emissions were linked to arriving trains
5) Another extended stationary sampling (6 h) for gravimetric analysis to calculate the specific density of PM used for the optical particle sizer (OPS) correction
6) Tracking of the differences in the dynamics of PM concentration between an old and a new type of subway train during the ride on the same track (line *U5*)

At the beginning and the end of each subway experiment, a minimum 20 min measurement walk (2 km) was taken between the university campus and the *NS-U/S* subway station to allow comparison with actual ambient urban PM levels. The mobile subway measurement routes (experiment 2 & 3) included train mid-section rides, stationary measurements simulating exposure of people waiting at selected platforms, and elevator rides. Platform measurements (experiment 4 & 5) were taken in the middle of the selected platform on designated passenger seats for the time necessary to obtain a sufficient number of data points. The operator documented the time at which trains entered and exited the station, and trains were categorized as old (o) and new (n), respectively. The *S-Bahn* platforms were measured similarly to *U-Bahn*. The investigation of the regional/long-distance train platform at the main station was conducted where most people gather and where small cafés and shops are also located. Sampling was done either cumulatively during the ride or at the selected platform (experiment 4).

Table 1
List of subway/train stations with abbreviations used in this study with average platform particulate matter (PMx), particle number concentration (PNC), equivalent black carbon (eBC) and UV-absorbing PM (UVPM) concentrations where the SD represents variability among measurements. For interpretation, design of the platform cross-section is indicated, where "P" is platform, "T" is track, "-" is direct transition and "|" indicate the separation of tracks/platform by a wall. Averages from ID 10-16 were not shown due to short measuring time.

ID	Name of the station	Abbr.	Lines	Type	Number of tracks (platform design)	PM_{10} (μg m^{-3})	$PM_{2.5}$ (μg m^{-3})	PM_1 (μg m^{-3})	PNC (pt cm^{-3})	eBC (ng m^{-3})	UVPM (ng m^{-3})	Size mode (nm)	No. of measurements
1	Neuperlach Süd	NS-U	U5, S7	overgr. (open w/ roof)	3 (T-P-T-T-P)	9 ± 5	3 ± 2	2 ± 2	7300 ± 7582	111 ± 117	620 ± 486	37 ± 19	7
2	Michaelibad	MC-U	U5	undergr.	2 (T-P-T)	59 ± 26	27 ± 14	9 ± 4	6547 ± 2419	4043 ± 1964	3236 ± 1353	40 ± 4	4
3	Ostbahnhof	OB-U	U5	undergr., transfer	2 (T-P-T)	205 ± 72	80 ± 18	21 ± 5	7470 ± 2773	9416 ± 3299	6840 ± 1694	43 ± 3	4
4	Odeonsplatz	OU-U	U4, U5	undergr., transfer	2 (T-P|P-T)	179 ± 52	70 ± 20	20 ± 6	6985 ± 1597	10540 ± 2628	6622 ± 1188	43 ± 2	4
5	Hauptbahnhof (over)	CS-U1	U4, U5	undergr., transfer	2 (T-P-T)	174 ± 40	66 ± 13	18 ± 4	8817 ± 2442	8648 ± 1469	6204 ± 562	40 ± 3	4
6	Hauptbahnhof (under)	CS-U2	U1, U2, U7, U8	undergr., transfer	4 (T-P-T-T-P-T)	220 ± 32	72 ± 7	20 ± 0.3	7175 ± 754	7845 ± 2560	6052 ± 723	46 ± 10	2
7	Hauptbahnhof Nord	CS-S	S1-4, S6-8	undergr., transfer	2 (P-T-P-T-P)	126 ± 89	42 ± 30	11 ± 7	6942 ± 1749	4616 ± 3053	3385 ± 2294	42 ± 7	4
8	Hauptbahnhof	CS-R	Railway	overgr. (semi-open), transfer	15 (large hall)	26 ± 9	11 ± 1	9 ± 1	7425 ± 4543	827 ± 401	1126 ± 707	48 ± 4	2
9	Innsbrucker Ring	IR-U	U2, U5	undergr., transfer	4 (T-P-T-T-P-T)	114 ± NA	48 ± NA	14 ± NA	5817 ± NA	7345 ± NA	5118 ± NA	46 ± NA	1
10	Therese-Giehse-Allee	TG-U	U5	undergr.	2 (T-P-T)	-	-	-	-	-	-	-	short
11	Neuperlach Zentrum	NZ-U	U5	undergr.	2 (T-P-T)	-	-	-	-	-	-	-	short
12	Quiddestrasse	QI-U	U5	undergr.	2 (T-P-T)	-	-	-	-	-	-	-	short
13	Max-Weber-Platz	MW-U	U4, U5	undergr.	2 (T-P-T-T-P-T)	-	-	-	-	-	-	-	short
14	Lehel	LH-U	U4, U5	undergr.	2 (T-P|P-T)	-	-	-	-	-	-	-	short
15	Karlsplatz (Stachus)	KA-U	U4, U5	undergr.	2 (T-P|P-T)	-	-	-	-	-	-	-	short
16	Theresienwiese	TW-U	U5	undergr.	2 (T-P-T)	-	-	-	-	-	-	-	short

2.3. Custom-built mobile measuring system

We developed a new mobile measurement system (Fig. S1 and full description in the SI) consisting of an actively ventilated, water-proof aluminum box with adjustable internal shelves, which serves as a housing for all online instruments and samplers. These are connected to omni-directional inlets (801565, TSI) by short conductive tubes. For underground measurements, the experimental box was attached to a frame rucksack, which was carried by the operator. While carried, the inlets in the breathing zone were at a distance of at least 20 cm from the operator to minimize personal cloud artifacts due to particles from clothing and hair (Licina et al., 2017). While riding the subway, the backpack was placed on a passenger seat, resulting in a measurement of the breathing zone of a seated person, similar to measurements on platforms. During reference ambient measurements, the box was secured in a modified stroller (Cab 2, Thule) to absorb vibrations. The temperature inside the box was kept within the operating range of the instruments to avoid discrepancies and extensive losses of volatile components from the samples.

2.4. On-line mobile measurements

PM size-distributions (OPS 3330, TSI) and PNC, the lung deposited surface area (LDSA) and size modes (DISCmini, Testo) were measured at 1 Hz resolution (0.2 Hz for OPS during platform measurements in one case), eBC and UVPM (MA200, Aethlabs; 150 mL min^{-1}, dual-spot) were measured at 0.1 Hz resolution. GPS coordinates were acquired at 1 Hz (64s, Garmin). Since GPS signal was not available in the subway, the time of door opening and closing was documented at each station with an accuracy of 1 s. All relevant events were noted or recorded with a cell

Table 2
Summary of on-line measurements (mean ± SD) of particle number concertation (PNC), particulate matter (PMx), lung deposited surface area (LDSA), equivalent black carbon (eBC), UV-absorbing PM (UVPM) and selected ratios during the sampling time for the metal analysis by ICP-MS for comparison. Routes B-F are described also in specific tables for each measurement based on the transects of the route (suppl. Tables S4–S10) to see the exact contribution of different environment.

Measurement	ID	Date	Duration	Start	Stop	PM_{10}	$PM_{2.5}$	PM_1	PNC	Size mode	LDSA	eBC	UVPM	$PM_{2.5}/PM_{10}$	$PM_1/PM_{2.5}$	eBC/UVPM
		DD-MM-YY	min.	hh:mm	hh:mm	μg m^{-3}	μg m^{-3}	μg m^{-3}	pt cm^{-3}	nm	μm^2 cm^{-3}	ng m^{-3}	ng m^{-3}			
Ambient walk 1	**A1**	19-10-21	91	15:35	17:06	16 ± 33	1.6 ± 1.0	0.9 ± 0.4	10352 ± 17752	37 ± 5	18 ± 10	371 ± 313	836 ± 325	0.1	0.5	0.4
Ambient walk 2	**A2**	26-10-21	74	14:21	15:35	8 ± 1	2.6 ± 0.8	1.2 ± 0.1	3262 ± 1373	47 ± 7	8 ± 3	401 ± 411	661 ± 443	0.3	0.5	0.6
Ambient walk 3	**A3**	26-10-21	67	15:46	16:53	9 ± 29	2.5 ± 0.7	1.1 ± 0.1	5963 ± 20012	53 ± 9	13 ± 11	31 ± 15	497 ± 266	0.3	0.4	0.1
Ambient walk 4	**A4**	27-10-21	81	7:50	9:11	15 ± 55	1.6 ± 1.7	0.7 ± 0.2	39615 ± 12525	22 ± 5	42 ± 10	1125 ± 751	1610 ± 755	0.1	0.4	0.7
Ambient walk 5	**A5**	27-10-21	77	9:25	10:42	15 ± 70	1.8 ± 1.9	0.7 ± 0.4	21653 ± 15180	29 ± 5	30 ± 11	NA ± NA	NA ± NA	0.1	0.4	NA
Ambient walk 6	**A6**	27-10-21	74	13:13	14:27	8 ± 17	1.8 ± 0.8	0.8 ± 0.1	5049 ± 1452	49 ± 3	14 ± 2	625 ± 437	709 ± 416	0.2	0.5	0.9
Subway scouting 1	**B**	04-11-21	97	7:17	8:54	137 ± 102	57 ± 39	17 ± 11	5550 ± 1922	41 ± 10	13 ± 5	7359 ± 5730	4659 ± 5015	0.4	0.3	1.6
Subway scouting 2	**C**	05-11-21	72	7:48	9:00	147 ± 119	51 ± 33	15 ± 8	12237 ± 5851	38 ± 6	24 ± 5	6906 ± 4445	4946 ± 2668	0.3	0.3	1.4
Subway scouting 3	**D**	17-11-21	101	8:47	10:28	109 ± 105	41 ± 32	14 ± 7	6998 ± 4236	44 ± 8	16 ± 7	4267 ± 4299	3369 ± 3074	0.4	0.3	1.3
Subway scouting 4	**E**	24-11-21	51	9:31	10:22	170 ± 71	59 ± 16	19 ± 4	6068 ± 2308	55 ± 5	19 ± 5	8423 ± 3624	5773 ± 2005	0.3	0.3	1.5
Subway route morning	**F1**	07-12-21	118	7:54	9:53	104 ± 89	41 ± 34	12 ± 9	6528 ± 3042	41 ± 7	14 ± 6	4560 ± 4313	3458 ± 2835	0.4	0.3	1.3
Subway route noon	**F2**	07-12-21	119	12:28	14:27	73 ± 58	29 ± 21	8 ± 6	5486 ± 2166	42 ± 8	13 ± 6	3707 ± 2913	3294 ± 2451	0.4	0.3	1.1
Subway route afternoon	**F3**	07-12-21	98	16:32	18:10	121 ± 82	45 ± 30	14 ± 8	13138 ± 6454	39 ± 5	27 ± 10	6022 ± 4402	4632 ± 2388	0.4	0.3	1.3
Platform sampling 1	**G1**	17-05-22	181	14:08	17:08	231 ± 52	96 ± 10	25 ± 3	6099 ± 630	56 ± 3	20 ± 1	8998 ± 2860	6919 ± 1499	0.4	0.3	1.3
Platform sampling 2	**G2**	19-07-22	164	20:36	23:20	218 ± 50	85 ± 8	26 ± 2	7857 ± 713	54 ± 3	25 ± 1	9967 ± 1153	7142 ± 772	0.4	0.3	1.4
Platform sampling 3	**G3**	28-08-22	360	14:06	20:06	181 ± 32	105 ± 24	29 ± 5	5074 ± 1111	64 ± 7	19 ± 2	5030 ± 608	4421 ± 478	0.6	0.3	1.1

phone camera for further data analysis. Temperature and relative humidity were measured sporadically by a data-logger with sensors (Almemo, Ahlborn or BiVOC2V2, Holbach).

The OPS was factory calibrated (TSI) with Polystyrene Latex (PSL) according to ISO 12501-1/4 and the dead time correction was used. As the density of the subway particles can differ significantly from the ambient air (Cha and Olofsson, 2018), corrections to the OPS were used for all measurements performed in the subway interiors and trains using gravimetric analysis by the external filter sampling (Section 2.5.1.). To avoid particle losses and minimize the time delay, the OPS was placed directly under the inlet.

Prior to each measurement, the instruments' flowrates were checked/calibrated using a mass flow meter (4043 H, TSI) as well as zero-filter checks (OPS), and automatic zero adjustments (DISCmini) were performed. The time was synchronized based on the GPS satellites.

2.5. Off-line measurements

For ICP-MS analysis, PM samples were collected on 47 mm quartz filters (preconditioned at 500 °C for 5 h) using the SG10-2 personal sampler (GSA) with a constant flowrate of 9 lpm and a filter holder with or without $PM_{2.5}$ pre-impactor (Sioutas, SKC; $PM_{2.5}$ or PM_{total}). The same filters were utilized for gravimetry prior to ICP-MS analysis. For quality assurance, two additional samples were taken simultaneously on 47 mm polycarbonate (PC) and 37 mm Teflon filters by additional SG10-2 samplers. For SEM-EDX analysis, BiVOC2V2 sampler (Holbach) with a constant flowrate of 2 lpm was used with a filter-holder and 47 mm PC filter, which also served as a support for 5 silica wafers (P-type boron dotted 5 × 5 mm). The samplers were calibrated using a mass flow meter (4043 H, TSI). Information on the filter material is given in Table S1 in SI. Time and duration of sampling are given in Table 3. Both blanks and field blanks were collected from each filter type.

2.5.1. Gravimetric analysis for correction of OPS data

Simultaneous 6h long sampling of $PM_{2.5}$ and PM_{total} for gravimetric analysis on three filter types (Section 2.5.) was performed on August 28, 2022 from 14:06 to 20:06 on the central part of the *U-Bahn* platform of the main train station *CS-U1* (line *U5/U4* with a 10 min interval on both lines). Filters were weighed prior and after sampling using a microbalance (Cubis MCA2.7S-2S00-F, Sartorius) and pre-conditioned (45% RH, 22 °C) for 24 h in a weighing chamber (pureGMC 18-EPA1065) with a corona discharge for filter deionization. All filters were weighed five times and the aerosol mass on the filter was calculated as the weight difference of the averages before and after the exposure. Then, the average 6-h PM mass concentration (μg m^{-3}) was calculated. For quality control, blank filters were weighed twice before and after exposure.

The OPS was measuring simultaneously at 0.2 Hz. The $PM_{2.5}$ mode from the entire sampling period was compared to the mode of gravimetric mass concentration from the PC, PTFE and quartz filter. The entire size range of the OPS from 0.3 to 10 μm (for underground measurements only) was then corrected by the correction factor:

$$OPS\ correction\ factor = \frac{c\ (g)}{c\ (OPS)} \quad (1)$$

where *c* (g) is the mass concentration of $PM_{2.5}$ from gravimetry and *c* (OPS) is the mode of $PM_{2.5}$ mass concentration from OPS.

2.5.2. Metal analysis using ICP-MS

Samples have been digested according to DIN 14902 (VDI 2267-part 15) by a Microwave speedwave ENTRY (Berghof) with a mixture of nitric acid (HNO_3, ultrapure grade, 69%) and hydrogen peroxide (H_2O_2, ultrapure grade 30%). Subsequently, samples have been diluted to a final volume of 50 mL with a final concentration of 5% of HNO_3. All the samples have been filtered utilizing a 0.2 μm syringe filter (Whatman Puradisc, 25 mm, 0.2 μm) and analyzed by Inductively Coupled Plasma

Table 3
Metal analysis by ICP-MS from mobile (A-G) and stationary (Ref) samples. Tables describing each transect and contribution of subway mobile measurements (B-F) are in the Supporting Information.

Measurement type	Reference ambient $PM_{2.5}$	Repetitions of the same ambient walk				Subway and railway scouting				Repetitions of a subway route at the same day			Subway platform stationary		Subway/ ambient
Route type/ stations	Station at UniBW	Urban PM background				NS-U, IR-U, OP-U, NS-U/S	OB-U, MC-U, NS-U/S	CS-U1, CS-U2, CS-R, OU-U	CS-U2, CS-U1, NS-U/S	NS-U/S, OB-U, OU-U, CS-R, CS-S, NS-U/S			CS-U1		Indoor/ outdoor ratio
ID	**Ref**	**A3**	**A4**	**A5**	**A6**	**B**	**C**	**D**	**E**	**F1**	**F2**	**F3**	**G1**	**G2**	**G1/Ref**
Sampling date	17-05-22	26-10-21	27-10-21	27-10-21	27-10-21	04-11-21	05-11-21	17-11-21	24-11-21	07-12-21	07-12-21	07-12-21	17-05-22	19-07-22	
Start sampling (hh:mm)	9:00	15:46	7:50	9:25	13:13	7:17	7:48	8:47	9:31	7:54	12:28	16:32	14:08	20:33	
Stop sampling (hh:mm)	9:00	16:53	9:11	10:42	14:27	8:54	9:00	10:28	10:22	9:53	14:27	18:10	17:08	23:21	
Sampling time (min.)	1440	67	82	78	74	97	72	102	51	118	119	97	180	168	
Sampled air (m^3)	641	0.60	0.74	0.70	0.67	0.88	0.65	0.91	0.46	1.07	1.07	0.88	1.53	1.43	
PM fraction	$PM_{2.5}$	PM_{tot}	PM_{tot}	PM_{tot}	PM_{tot}	PM_{tot}	PM_{tot}	PM_{tot}	PM_{tot}	PM_{tot}	PM_{tot}	PM_{tot}	$PM_{2.5}$	PM_{tot}	$PM_{2.5}$
Fe (μg m^{-3})	**0.073**	**2.6**	**1.6**	<LOQ	<LOQ	**115**	**123**	**20**	**122**	**56**	**49**	**91**	**67**	**171**	**911**
Mn (ng m^{-3})	**12.6**	**35**	**28**	**28**	<LOQ	**1045**	**1123**	**177**	**1113**	**523**	**503**	**804**	**617**	**1560**	**49**
Cr (ng m^{-3})	**1.2**	**205**	**159**	**154**	**180**	**420**	**448**	**151**	**786**	**306**	**215**	**384**	**197**	**484**	**163**
Cu (ng m^{-3})	**2.8**	**250**	**143**	**113**	**117**	**641**	**577**	**120**	**651**	**439**	**357**	**635**	**262**	**534**	**95**
Ni (ng m^{-3})	**0.51**	**232**	**73**	**57**	**109**	**317**	**308**	**76**	**683**	**206**	**141**	**245**	**146**	**344**	**286**
V (ng m^{-3})	**0.10**	<LOQ	<LOQ	<LOQ	<LOQ	<LOQ	<LOQ	<LOQ	<LOQ	<LOQ	<LOQ	<LOQ	<LOQ	**31**	NA
Pb (ng m^{-3})	**0.90**	**24**	**25**	**22**	<LOQ	<LOQ	<LOQ	<LOQ	**44**	**16**	<LOQ	**16**	<LOQ	**9**	NA
Mn to Fe (%)	17	1.3	1.8	NA	NA	0.91	0.91	0.89	0.91	0.93	1.03	0.88	0.92	0.91	
Cr to Fe (%)	1.7	7.9	9.9	NA	NA	0.37	0.36	0.76	0.64	0.55	0.44	0.42	0.30	0.28	
Cu to Fe (%)	3.8	9.6	8.9	NA	NA	0.56	0.47	0.60	0.53	0.78	0.73	0.70	0.39	0.31	
Ni to Fe (%)	0.7	8.9	4.5	NA	NA	0.28	0.25	0.39	0.56	0.37	0.29	0.27	0.22	0.20	

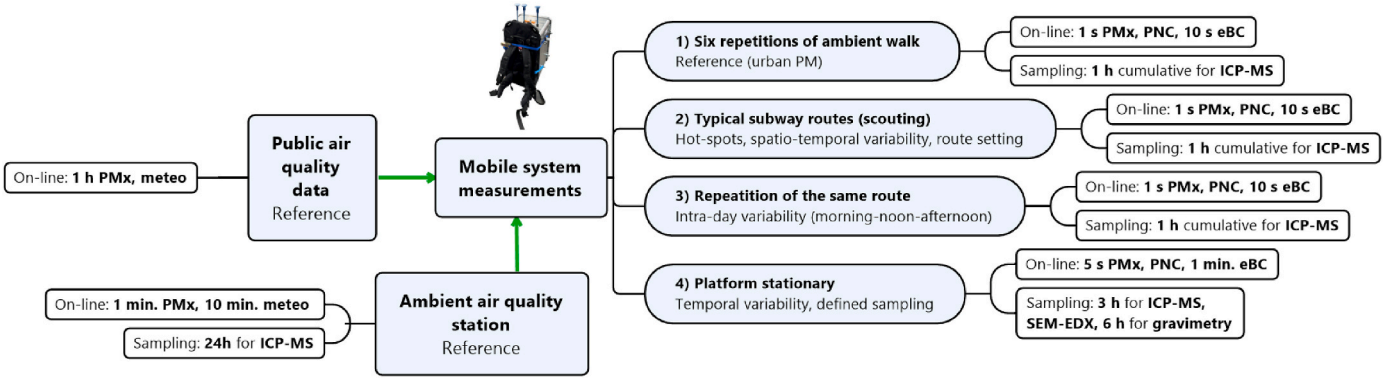

Fig. 1. Strategy of measurements and sampling of the subway micro-environment using the mobile measuring system; PNC, particle number concentration; PM, particulate matter; eBC, equivalent black carbon; ICP-MS, inductively coupled plasma mass spectrometry.

Mass Spectrometry (ICP-MS, Agilent Technologies 8900). Calibration standard curves for all measured elements were used for the quantification, as well as for the calculation of limits of detection (LOD) and quantification (LOQ). Three technical replicates have been performed for each sample, field and method blank. To check the extraction efficiency on each sample, prior to the digestion, a spike with a concentration of 20 μg L^{-1} of internal standard mix for ICP-MS systems was added. The constancy and the correctness of the analytical values of the used internal standard (ISTD) were checked in time through a control chart that documents the trend of the ISTD values.

2.5.3. Imaging and single particle elemental analysis using SEM-EDX

Samples used for analysis via SEM-EDX were stored in a desiccator under vacuum for 24 h to ensure removal of volatile components. Afterwards, 12 mm circular punches were cut from 47 mm PC filters, which were then transferred to 12 mm SEM pin stub sample holders with EDX suitable adhesive carbon pads in between. To minimize charging effects, the surface of the filters was coated in a Q150T ES Plus sputter device (Quorum technologies) with a thin carbon layer utilizing a woven carbon fiber string in pulsed cord evaporation mode.

Particles collected from subway stations were imaged with the built in Inlens and SE2 detectors of a Gemini Sem 360 (Carl Zeiss). EDX analysis was conducted with an Ultim Max 40 detector (Oxford instruments) at the optimum detector working distance of 8.5 mm. Usage of a silicon drift detector with a thin detector window ensured suitability for analysis of low-Z elements ($Z > 6$) such as C and O. The EHT was set to 5 kV for particles smaller than 0.5 μm to reduce the interaction volume of the beam, thus minimizing total passage of the beam through the particles with subsequent excitement of underlying materials such as the PC filter. Larger particles were measured with either 12 kV (particle sizes from 0.5 to 2.5 μm) or 20 kV acceleration voltage (particles >2.5 μm). Semi-quantitative EDX data was recorded for over 180 000 particles, followed by automated classification based on their main contributing elemental concentrations.

2.6. Reference stationary PM sampling and measurements

An air quality station on the university campus (GPS: 48°04′37.5″N 11°38′21.2″E) served as a reference for the subway measurements. A high-volume sampler (DHA-80, Digitel) with a $PM_{2.5}$ sampling head and a flowrate of 500 lpm was used to compare elemental composition between ambient air and in the subway. Daily 24-h samples starting at 9 a.m. were collected on 150 mm filters (Whatman QM-A, pre-conditioned for 5 h at 500 °C). PM size-distribution with 1 min time-resolution (APDA-372, Horiba with the Sigma-2 sampling head complying with VDI 2119-4, $PM_{2.5}$ according to EN14907 and PM_{10} EN 12341) and a weather station with 10 min data acquisition (Vantage 2 Pro, Davis) supported the interpretations.

2.7. Data analysis

On-line raw data were manually checked for potential errors caused by mobile use of instruments and processed in the manufacturer's software. PNC data from DISCmini were corrected for induction effects and cross-checked against a CPC (5416, Grimm) prior to the campaign. OPS data were corrected (see chapter 3.5.1.). BC and UVPM data (MA200, AethLabs) were smoothed using the Optimized Noise-reduction Averaging (ONA) algorithm with a smoothing factor of 0.01 (Hagler et al., 2011; Liu et al., 2021; Ji et al., 2022). When GPS signal was available, PNC and PM data were merged together with the GPS coordinates and plotted on maps using ArcGIS Pro software (ESRI). ICP-MS and SEM-EDX data were processed with the manufacturer's software.

3. Results and discussion

3.1. Reference ambient PM measurement (stationary and mobile)

For comparison with subway measurements, the average ambient concentrations of PM_1, $PM_{2.5}$ and PM_{10} on the university campus in May 2022 were 6 ± 4, 7 ± 4, 11 ± 5 μg m^{-3}, in July 2022 5 ± 3, 6 ± 4, 12 ± 7 μg m^{-3}, and in August 2022 5 ± 2, 7 ± 3, 11 ± 6 μg m^{-3}, respectively. At the same time, $PM_{2.5}$ values measured at the background station of the Bavarian Monitoring System for Air Quality (LÜB) in *Johanneskirchen* (Munich; *https://www.lfu.bayern.de/luft/immissionsmessungen/*), were 8 ± 4, 9 ± 4 and 9 ± 4 μg m^{-3} in May, July and August 2022, respectively. In October, November and December 2021, the $PM_{2.5}$ concentration in *Johanneskirchen* were 7 ± 4, 6 ± 5, 5 ± 5 μg m^{-3}, respectively. In summary, $PM_{2.5}$ levels on the campus were slightly lower than in the city. This confirms our reference site and its classification as an urban background station.

Six repetitions of the identical 1-h route in the vicinity of the station *Neuperlach Süd* (*NS-U/S*, see Fig. S2 with a detailed description in the SI) were used as comparison with the subway measurements (Fig. 4). They showed relatively high ambient spatio-temporal variability in PNC (Table 2) with the main road as the dominant source. Traffic strongly contributed to PNC values at the above-ground *U5* terminus *NS-U/S*. PNC were highest during the morning rush-hour (Ambient walk A4 and A5) and lowest in the early afternoon when traffic was reduced (A2, A6). According to DISCmini, the size mode ranged between 22 and 53 nm. PM_1 dynamics did not follow the PNC trend because ultrafine particles contribute little to the total mass concentration due to their low mass per particle. Furthermore, the OPS size range started at 300 nm. The PM_1/$PM_{2.5}$ ratio was similar for all 6 routes (0.4–0.5), which could indicate the same/similar dominant source of fine particles. PM_{10} had high SD (noise) due to the 1 Hz acquisition time and greater dynamics. Average eBC value between walks was 511 ± 417 ng m^{-3} and average ultraviolet

absorbing PM (UVPM) was 863 ± 525 ng m^{-3} with the highest value of 1.6 μg m^{-3} on October 27, when PNC was also highest. Since UVPM is an indicator of wood smoke and the measurements were taken during the heating season, domestic heating could contribute to the elevated background concentrations. The eBC/UVPM ratio was 0.7 on this day, otherwise, it varied from 0.1 to 0.9 between walks. The results of metal analysis by ICP-MS from the cumulative sampling can be found in Section 3.5.

3.2. Corrections of on-line subway measurements using gravimetry

The average $PM_{2.5}$ mass concentrations at the *CS-U1* platform (August 28, 2022, 14:06-20:06) calculated from PC, PTFE and quartz filters (simultaneous sampling) were 100.2 ± 4.13, 103.2 ± 1.65 and 102.9 ± 5.66 μg m^{-3}, respectively, with a median of 102.9 μg m^{-3}, whereas the $PM_{2.5}$ median measured on-line by the OPS was 48.8 μg m^{-3} (with a preset density 1 g cm^{-3} and default refractive index). Therefore, the correction factor of 2.11 from both medians was determined. This should roughly correspond to the average effective density of $PM_{2.5}$ in g cm^{-3}. However, as aerosol composition and particle structure vary over time, place and particle size, a more detailed measurement of effective density would be beneficial for precise correction. This aspect should be considered while comparing absolute values from on-line optical PM instruments among different studies but also within the same subway system due to different micro-environments. In Stockholm, precisely measured subway particle effective density was 1.87 ± 0.22 g cm^{-3}, which is in a similar range (Cha and Olofsson, 2018), however, the correction factors in Athens, Barcelona and Oporto suggest that there is high variability among subway systems (Martins et al., 2016), probably also in effective densities. One of the reasons could be different relative contributions of subway generated particles to PM e.g., due to different air exchange rates with the ambient environment and/or different emission patterns. During the same time, the PM_{total} concentration was 209.0 ± 7.79 μg m^{-3} (gravimetry) resulting in $PM_{total}/PM_{2.5}$ ratio of 2.1 (assuming zero sampling losses). Based on the corrected OPS, the PM_{10} concentration was 181 μg m^{-3} implying that particles larger than 10 μm in size should contribute about 28 μg m^{-3} to the PM_{total}. As a result, $PM_{2.5}/PM_{10}$ ratio was 0.6, PM_1/PM_{10} was 0.2, and $PM_1/PM_{2.5}$ was 0.3. The sampling was done on Sunday, however, the number of persons on the platform was comparable to weekdays (not quantified).

3.3. On-line PM subway measurements – general overview

Table 1 summarizes the average concentrations of PM, PNC, eBC and UVPM at selected underground and overground platforms of the *U-Bahn, S-Bahn* and railway main train station from all our measurements and lists the station abbreviations used in the figures.

The lowest PM mass concentrations were measured at *Michaelibad* (*MC-U*) with PM_{10}, $PM_{2.5}$, PM_1 = 59 ± 26, 27 ± 14, 9 ± 4 μg m^{-3}, respectively. The highest average concentrations were at the deeper *U-Bahn* platform of the *Hauptbahnhof* transfer station (*CS-U2*) with PM_{10}, $PM_{2.5}$, PM_1 = 220 ± 32, 72 ± 7 and 20 ± 0.3 μg m^{-3}, respectively. These values are concerning when compared to the WHO Air Quality Guidelines values of daily PM_{10} and $PM_{2.5}$ for outdoor air.

Table 2 shows the comparison between the different mobile and platform measurements, where **A1-A6** are repetitions of ambient walks, **B-E** are subway scouting trips, **F1-F3** are repetitions of the same ride in the morning, midday and afternoon, and **G1-G3** are several hours long stationary measurements on the *CS-U1* platform. The highest concentrations of PM_{10}, $PM_{2.5}$, PM_1 = 231 ± 52, 96 ± 10, 25 ± 3 μg m^{-3}, respectively, were recorded during the 3h long stationary measurement on May 17. This was in a similar range as at the Prague transfer station *Muzeum* with 214.8, 93.9 and 44.8 μg m^{-3} of PM_{10}, $PM_{2.5}$, PM_1, respectively (Cusack et al., 2015), however, the PM_1 in Munich was 2.3 times lower. The reason could be a lower contribution of ambient traffic-related particles to PM_1, which could be caused by both the reduced nearby traffic sources in Munich and/or lower air exchange with outside air (ventilation). This hypothesis is supported by the PNC values (Table 2, Fig. 4), which are, on average, at a similar level to the ambient urban background. This is also valid for LDSA and size-mode, both measured in the range of 10–300 nm and associated with PNC. $PM_{2.5}/PM_{10}$ ratio in the subway ranged from 0.4 to 0.6 and is higher than for ambient air (see Section 4.2.). Based on reviews of Carteni (Cartenì et al., 2020) and Chang (Chang et al., 2021) on subway PM in other cities, the highest average PM_{10} and $PM_{2.5}$ concentrations of 470 μg m^{-3} and 260 μg m^{-3}, respectively, were recorded on the platform in Stockholm in 2000 (Johansson and Johansson, 2003). In Rome in 2005, PM_{10} was 409 ± 22 μg m^{-3} (Perrino et al., 2015). High PM_{10} values were also observed in Seoul, Barcelona, Paris, Beijing, Milan, Budapest, Athens and other cities, while relatively low concentrations were determined in Naples, Sydney, and Turin (Cartenì et al., 2020).

The mean eBC concentration at the *CS-U1* platform was 8.0 ± 2.6 μg m^{-3} (**G1-G3**) and mean UVPM 6.2 ± 1.5 μg m^{-3}, which was significantly higher than in ambient air (during ambient walks **A1-A6** the mean eBC was 0.5 ± 0.4 μg m^{-3} and the highest values 2.5 ± 1.5 μg m^{-3} were recorded on December 7. 2021). Both eBC and UVPM correlated with PM measured by OPS. For comparison, in subway in Sao Paolo eBC were 11.33 ± 12.98 μg m^{-3} (Targino et al., 2021), in Helsinki 6.3 ± 1.8 μg m^{-3} (Aarnio et al., 2005), and in Montreal 4.6 ± 2.3 μg m^{-3} (van Ryswyk et al., 2017). Sources of BC are typically linked to combustion processes (e.g. diesel emissions), however, since we observed only minor amounts of soot-agglomerates via SEM in the Munich subway, we hypothesize that most of the eBC readings is caused by the interference of light absorbing iron oxide particles, which we identified as the major source of aerosol mass based on results from ICP-MS (Section 3.5.) and SEM-EDX (Section 3.6.). Moreover, PNC levels in the subway also suggested low intake of traffic related particles. Other sources of carbonaceous particles in the subway could be disc brake abrasion, as graphite is added to brake discs as a lubricant (Lyu and Olofsson, 2020), and carbon from electric motor brushes (Font et al., 2019). However, based on our SEM-EDX and ICP-MS analysis of trace elements typical for brake emissions, this cannot explain all eBC readings. Nevertheless, as the micro-aethalometer values correlated with the subway-PM measured by OPS, it was a good indicator of PM hot-spots. The possibility of micro-aethalometer artifacts in the subway has already been discussed (Midander et al., 2012; Targino et al., 2021) and we expect that interferences might affect published results from other subway studies. Therefore, this topic should be the subject of further investigation.

3.3.1. Subway scouting: hot-spots identification, effect of platform design on PM

Scouting rides (Table 2, **B-E**) represent various common trips of about 1h in the Munich subway system in November 2021 (same season as the reference ambient walks). As each of these routes was different, the exact routes are listed in SI (Tables S2–S8) with mean values of PM_{10}, $PM_{2.5}$, PM_1, PNC, eBC and UVPM for each transect (where the ambient walk is *aw*, the indoor walk *iw*, the subway ride *r*, and the platform stationary is *s*). The time of cumulative personal sampling for ICP-MS (section 3.5.) is marked in bold.

Based on these data, hot-spots were identified as transfer stations with higher train frequencies. The highest PM_{10} average values from repeated measurements (Table 1) were measured at *CS-U2,* the deepest of the *U-Bahn* platforms with values of 220 ± 32 μg m^{-3}, while the *U-Bahn* station *CS-U1* located above this platform, had an average concentration of 174 ± 40 μg m^{-3}. The depth of the station may play a role (Cartenì et al., 2015) but number of trains, station design (Table 1) and eventually ventilation seem to be responsible for the differences. *CS-U2*, with its four tracks not-separated by a wall, allows for a greater volume of mixing air compared to *CS-U1* with two tracks. The total train frequency is similar, but the peak-hour frequency at *CS-U2* is nearly twice as high. However, even with the same actual train frequency, PM_{10} concentrations at the *CS-U2* station were higher than at *CS-U1*

(Table S4). An interesting comparison is between the *U-Bahn* transfer station *Innsbrucker Ring* (*IR-U*, Table S2) with the lowest observed PM_{10} (114 μg m^{-3}, only one measurement) and *CS-U2* with the highest PM, which has almost the same platform design. Given that the difference in PM_{10} was approximately a factor of two when measured with similar actual train frequencies (Table S2, Table S4), it appears that *IR-U* is better ventilated. To investigate the difference in PM between two-track platforms, we compared *U-Bahn* station *Odeonsplatz* (*OU-U*, 179 ± 52 μg m^{-3}) with two tracks separated by a wall and *U-Bahn* station *CS-U1* with the shared platform mentioned above. As seen in Table 1, no significant difference in PM was observed. The measurements for these comparisons were not done simultaneously, but based on the standard deviations of repeated measurements at different times and even seasons, the concentrations were relatively stable. However, more measurements would be needed to accurately quantify the differences. Additional CO_2 measurements would help to investigate the effect of ventilation on PM. Another important hot-spot among the investigated routes was the *U-Bahn* transfer station *Ostbahnhof* (*OB-U*, 205 ± 72 μg m^{-3}), where $PM_{2.5}$ and PM_1 reached 80 ± 18 μg m^{-3} and 21 ± 5 μg m^{-3}, respectively. The busy *S-Bahn* underground station *Hauptbahnhof (CS-S*, a two-track platform with extended platforms on both sides of the tracks) yielded PM_{10} 236 ± 52 μg m^{-3} in the scouting measurement on November 24, 2021, but the mean value of the other investigations was 126 ± 89 μg m^{-3} and the lowest measured PM_{10} of 34 ± 21 μg m^{-3} on December 7, 2021 (Table S6). The neighboring *U-Bahn* stations *CS-U1* and *CS-U2* showed higher PM concentrations even at lower train frequencies. Because *S-Bahn* trains exit the tunnel to the surface 200 m beyond the *CS-S* station, it is probably better ventilated. More measurements would be needed to compare, which train emits/resuspends more particles.

In summary, the recommended PM levels for ambient air by the WHO (World Health Organization, 2021) were exceeded at almost all measurement sites and are, therefore, high for long-term exposure.

3.3.2. Repetition of the same route: intra-day variability, indoor/outdoor comparison

Based on the subway scouting rides (section 3.3.1.), a route was defined for repeated measurements. The heat-map (Fig. 4) summarizes the on-line measurements of the repetitions of the same route in the morning (*m*), noon (*n*) and afternoon (*a*) and shows how many times the concentrations of PM_1, $PM_{2.5}$, PM_{10}, PNC, eBC and UVPM were elevated on the specific transect of the route (x-axis) compared to the average concentrations of the reference ambient routes (section 3.1.). Ambient walking measurements (*aw*) at the beginning and end of each route show the deviation from the reference ambient measurement at a given time. Stationary measurements at selected platforms (*s*) and subway rides (*r*) are located between the dashed vertical lines indicating train boarding and exiting.

Generally, PM concentrations were highest during the morning and afternoon rush-hours and lowest during midday. Train frequency was a key factor, as it was 5 min in the morning (7-9 am) and afternoon (3-7 pm) rush-hours and 10 min during noon, which corresponds with measured PM (the morning measurement period occurred between 7:54-9:53 and the afternoon period between 16:32-18:10). Other factors may contribute to intra-day variability, such as the number of people moving on the platform, as discussed e.g. in the Shanghai study (Zhao et al., 2017).

At the stations (*s*) measured, the highest PM concentrations were generally at transfer stations with more lines and thus higher overall train and passenger frequencies. $PM_{2.5}$ concentrations at *OB-U* station were 44 times higher than ambient urban background levels. During the ride, the PM concentrations were usually greater in the tunnel than on the platforms. This was observed also in Prague (Braniš, 2006), but not in Barcelona (Martins et al., 2015). The tunnel was found to be a dominant source of PM and the quality/lack of train ventilation influenced how much PM entered the trains. Similar findings have been reported in Athens (Martins et al., 2016) and Naples (Cartenì et al., 2015). At *S-Bahn* platforms the PM concentrations were lower than at *U-Bahn* platforms as well as during *S-Bahn* trips. As discussed in Section 3.3., PNC inside trains and on platforms were generally at ambient levels. On elevators, all PM concentration decreased to the half while PNC values increased suggesting that there is a sufficient air exchange with the outside, which is more polluted by traffic in the city center.

To compare personal exposure, average time periods spent at the platforms and in the trains as well as average human breathing rates would need to be considered. In Barcelona, concentrations were higher at platforms, however, based on their calculations, the dose was double in trains due to the longer exposure time (Martins et al., 2016).

From the heat-map in Fig. 4, it is visible that spatial variability of PM is more important than temporal and the PM concentrations are raising when travelling from open-space terminus *NS* to the city.

Because no emissions from combustion processes have been observed at the majority of platforms, eBC and UVPM readings are most likely FePM interferences, as discussed in Section 3.3. However, the MA-200 instrument can explain the PM spatio-temporal variability similar to OPS. As the MA-200 has a suitable size for mobile measurements, its use for identifying hot-spots might be interesting and more detailed analysis of eBC and UVPM might be part of a future study.

3.3.3. Micro-scale PM spatio-temporal variability during the specific rides, old vs. new trains

Exemplarily, Fig. 2 shows the detailed variability of PM and PNC in 1 Hz resolution with a 10 s moving average (line). It represents the typical ride from the terminus *NS-U/S*, which is over-ground so ambient urban PM and PNC concentrations were present at the station and inside the train. This represents an ideal start for investigating the dynamics of concentrations inside the train and the behavior of PM in the tunnel system.

PM_{10} concentrations started to raise when the train entered the tunnel and reached about four times higher values within only 1 min until the next stop. The rapid exchange was accelerated by open windows in the wagon of the "old" train, which was empty. PM concentrations increased relatively uniformly throughout the entire ride to downtown. In less than 20 min, PM_{10} reached up to one order of magnitude higher levels at *U-Bahn* station *CS-U1* (city center). Opening the doors at the stations (indicated by vertical lines) typically caused an immediate slight decrease in PM_{10} concentrations as the air was exchanged and diluted. The largest decrease occurred at the *U-Bahn* station *IR*, which has an exceptionally large size and relative low concentration levels, as discussed in Section 3.3.1. The station itself did not serve as a significant sink for PM_{10} from the tunnel since concentrations rose sharply up- and downstream of the *IR* platform.

$PM_{2.5}$ and PM_1 were increasing gradually (slightly step-wise) with a similar trend, but the overall dynamics were lower with concentrations up to about 100 and 25 μg m^{-3}, respectively. PM_1 remained stable and the effects of the stations were negligible.

PNC did not follow the trend of PM and remained mostly at urban background levels, as shown previously (Table 2, Fig. 4). At the *U-Bahn* station *Neuperlach Zentrum* (*NZ-U*), PNC were around 11 500 pt cm^{-3}, which is appr. twice as high as the usual values in the *U-Bahn*. Most likely, traffic related particles were introduced into the subway system, since there is a large bus station, a shopping mall, and a relatively busy street above the *NZ-U* station. Interestingly, PNC were already rising at the previous subway stop. A similar situation on a smaller scale occurred at the next stop *U-Bahn* station *Quiddestrasse* (*QI-U*), and thereafter, the PNC decreased to "normal" levels within 2 min of travelling, while $PM_{2.5}$ continued to increase. The lower PNC in tunnels and stations in the city center might be caused by the lack of ventilation rather than absence of traffic-related particles above the subway.

The same experimental route was repeated with a new train (*n*) with air conditioning and closed windows (Fig. S6). First, on the way from *CS-U1* to the terminal station *NS-U/S* and then, after a short brake, back to the *CS-U1* platform with exactly the same train. The average

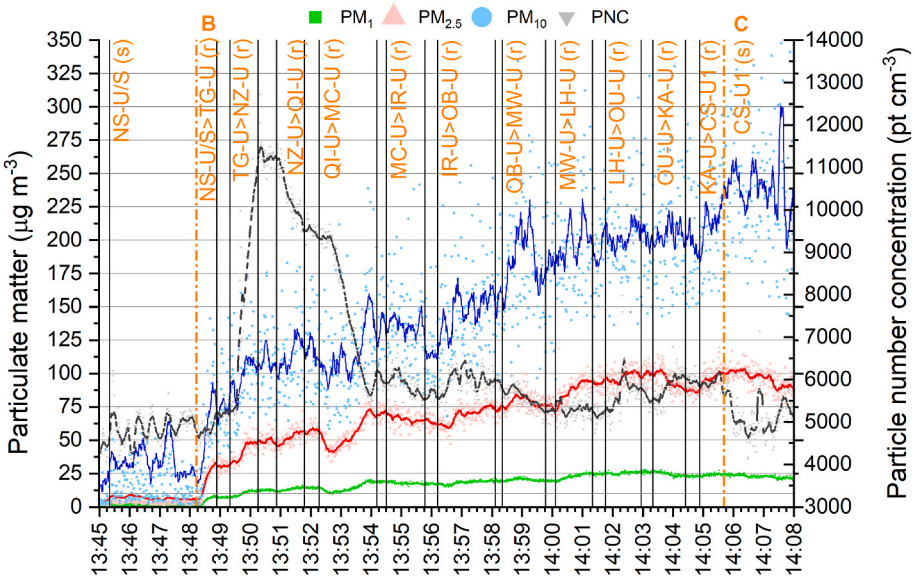

Fig. 2. PM_1, $PM_{2.5}$, PM_{10} and particle number concentration (PNC) dynamics during the ride (B) from the over-ground subway terminal station NS-U/S towards CS-U1 station by the old train (U5 line) on 17. 5. 2022. First vertical black line represents entering the train, which was waiting in the station (s), orange dashed line entering the tunnel and following black lines indicate door opening/closing at the stations (stations' abbreviations are above with indication of the direction of the ride (r), list of abbreviation is in the Table 1). Scatter represents 1s dynamics of concentrations and color lines are 10s moving averages. PM_x data of the part B and C were corrected based on the effective density of $PM_{2.5}$ (2.106 g cm^{-3}) measured at CS-U1 on 28. 8. 2022.

concentrations of PM_1, $PM_{2.5}$, PM_{10} were only 8-10% higher on the way from *CS-U1,* PNC were 2% higher. After the 40 min measurement at *CS-U1*, the same route to *NS-U/S* was repeated by an old train (o). Surprisingly, the difference in dynamics between old and new train in the same direction was only 7-12% for PM_1, $PM_{2.5}$, PM_{10} and 13% for PNC. The air conditioning systems seemed to be not efficient enough or were not equipped with air filters, which would clean the indoor air. Therefore, the air conditioning systems should be improved to achieve higher filtration efficiencies, such as in Barcelona (Querol et al., 2012).

3.4. PM dynamics on subway platforms during stationary measurements

As described in Section 4.2. and 4.3., PM concentrations measured stationary at the *U-Bahn* platform *CS-U1* were relatively stable in the range of 10^2 µg $m^{-3}$of PM_{10} (Table 2, Fig. 4). PM and PNC were illustrated in Fig. 3, which shows a 42-min representative section in order to investigate the source and what might influence the micro-dynamics. The columns indicate the time the train was in the station (*U5* in brown, *U4* in green), the arrow indicates the direction of travel (left: *Laimer Platz to Theresenwiese*, right: direction *NS-U/S to Arabellapark*).

Significant signals of PNC were associated with high numbers of people exiting the train (e.g. at 14:13-14:14), but the exact number was not noted. The signal decrease occurred relatively fast after departure of the train due to the wind caused by train movement (piston effect). The movement of the train is also affecting PM, probably due to the entering of polluted air from the tunnel. A similar behavior was described e.g. in Barcelona (Moreno et al., 2014). In some cases, when two trains left at the same time but in opposite directions (e.g. time 14:42-14:43 and 14:35), the PM_{10} concentration raised rapidly for a short time. In this

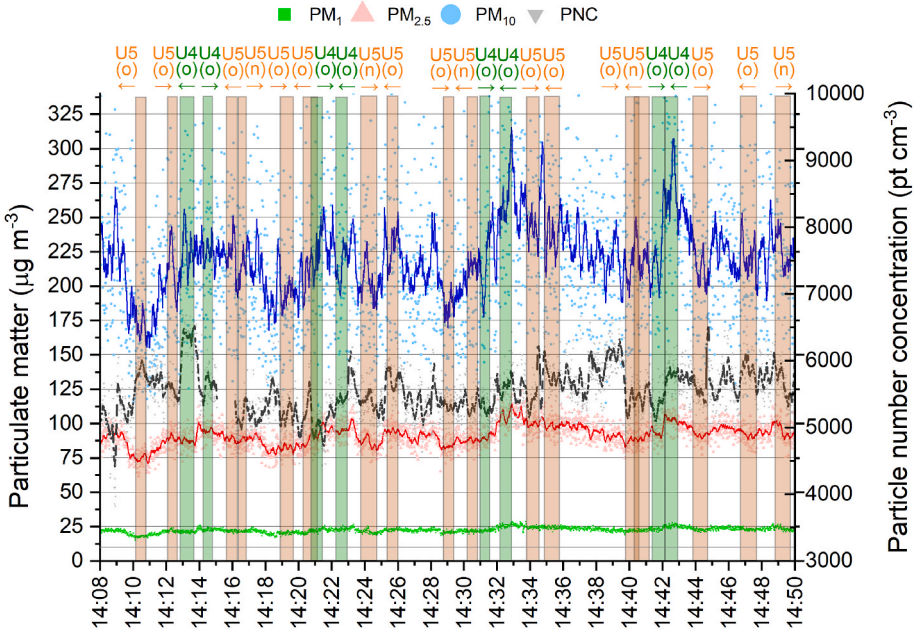

Fig. 3. Dynamics of PM_1, $PM_{2.5}$, PM_{10} and particle number concentration PNC (1s scatter) with 10s moving averages (color lines) at the Munich U4/U5 subway station CS1-U on 17. 5. 2022. Columns indicate trains in the station (arrival-departure), the line U4 (green) and U5 (brown) and the direction is indicated above (right arrow is towards NS U5/Arabelespark U4 station), "o" indicates the old train and "n" the new train.

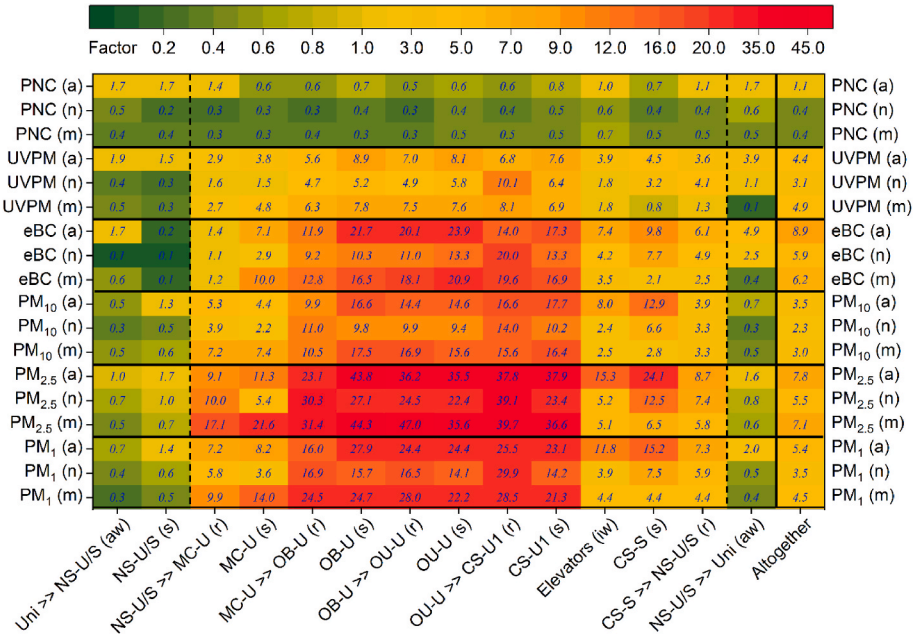

Fig. 4. Spatio-temporal variability of PM_1, $PM_{2.5}$, PM_{10}, equivalent black carbon (eBC), UV-absorbing PM (UVPM), particle number concentration (PNC) during the repetition of the same route in the morning (m), noon (n) and afternoon (a) on 12. 7. 2021. Each route is divided into ambient walk (aw), indoor walk (iw), stationary measurements at platforms (s) and rides by the train (r). Dashed line indicates entering and exiting the train. Heatmap represents the ratio of the average absolute concentrations of each part of the route to the overall average of 6 repetitions of a typical ambient walk (urban PM background) around the NS-U/S station. Last column "Altogether" represents the average from the whole route. Route starts and finishes at the campus of the Bundeswehr University (Uni) and consist of underground (U) and overground (S) stations listed in Table 1.

experiment, there was no significant difference in PM concentrations between new and old trains. Most likely, both trains resuspended PM similarly and any possible difference in emissions did not appear on the platform.

3.5. ICP-MS metal analysis

Table 3 shows the results of ICP-MS analysis for personal samples from 4 typical ambient walks (**A3-A6**) and 24-h reference stationary ambient air sampling using a high-volume sampler for comparison (**Ref**), 4 scouting subway routes (**B-E**), 3 repetitions of the same route (**F1-F3**), and two stationary platform measurements (**G1, G2**). All samples contain the PM_{total} fraction except **G1** and **Ref**, where it is $PM_{2.5}$. All routes are described in the previous chapters (Table 2 contains corresponding averages from on-line instruments) and additional parameters are available for comparison (Table 1, Tables S2–S8). In addition to Fe, Mn, Cr, Cu, Ni, V and Pb listed in Table 3, other elements were analyzed of which Na, Al, K, Zn and Ba were excluded from the dataset due to high blank concentrations. The reason for this could be the short sampling time, contamination and/or use of quartz filters. For other elements (Be, Mg, V, Co, As, Se, Ag, Cd, Sb and Th), both blanks and all samples were below the limit of detection (LOQ). This may be due to short sampling times and/or low concentrations in the air.

During the subway scouting rides, the highest concentrations of iron (Fe) in the PM_{total} fraction of 123 μg m^{-3} was recorded on November 5, 2021, while the highest concentration during the ambient walks was 2.6 μg m^{-3} on October 26. 2021. Fe was the dominating metal in the subway, as in other subway systems (Font et al., 2019; Chang et al., 2021; Ji et al., 2021). Subway scouting routes **B-E** yielded similar values with the exception of route **D**, which contained 48-min. measurements at the railway main train station (*CS-R*, Table S4). PM concentrations on the *CS-R* platform were close to ambient levels probably due to good ventilation. The Fe content per average aerosol mass followed a similar trend in all subway samples (on average about 1.7 compared to 0.2 in the ambient air). Further abundant metals were manganese (Mn), chromium (Cr), and copper (Cu). A significant increase in the subway was also observed for vanadium (V), however, most of the filters were below the LOQ.

Stationary measurements on the U-Bahn platform *CS-U1* revealed an Fe concentration of 67 μg m^{-3} in the $PM_{2.5}$ fraction on May 17, 2022 accounting for about 69% of $PM_{2.5}$ (Table 2). On July 19, 2022, the Fe concentration in PM_{total} was 171 μg m^{-3} while PM_{10} and $PM_{2.5}$ fractions were 218 ± 50 μg m^{-3} and 85 ± 8 μg m^{-3}, respectively. Therefore, most of the PM mass was formed by ferruginous particles (FePM).

The ratio of iron to other metals could provide information on the origin of the particles if compared to the corresponding ratios in materials subject to abrasion. The Mn/Fe ratio was 0.01 as in the Barcelona subway, where it was considered as a typical ratio for the origin of steel from wheels, rails and brakes (Moreno et al., 2015). The average ratios of different metals compared to Fe at *CS-U1* platform were 0.91% (Mn), 0.39% (Cr), 0.45% (Cu), 0.30% (Ni), 0.018% (V), respectively, while the usual composition of one of the most common rail steel R260 is: 0.92–1.07% (Mn), 0.03–0.12% (Cr), 0.01–0.12% (Cu), 0.01–0.08% (Ni), 0.002–0.011% (V), respectively. The variation for some elements may be due to the contribution of other sources or slightly different steel types used. Cu, Mn, Cr, and Ni are present in brake pads (with high variance), which are subject to wear (Font et al., 2019).

3.6. SEM-EDX imaging and single particle elemental analysis

The majority of subway particles analyzed via SEM exhibited a rough, splintery surface, oftentimes present as flakes (exemplary micrographs of characteristic particles are shown in Fig. 5a and Figs. S8-11Figs. S7–10 in the SI), which is in agreement with results of studies all over the world (Jung et al., 2012; Loxham et al., 2013; Moreno et al., 2015; Perrino et al., 2015; Wang et al., 2016; Grana et al., 2017; Chang et al., 2021; Guseva Canu et al., 2021). The uneven and rough edges found for most particles suggest that they are mainly derived from abrasion processes, most likely at the rail-wheel-brake interface (Kang et al., 2008; Byeon et al., 2015; Moreno et al., 2015; Perrino et al., 2015; Wang et al., 2016).

EDX analysis revealed that these particles consist predominantly of Fe (63.4 ± 8.67 wt%) and O (36.2 ± 8.2 wt%), with lower contents of Si (0.1 ± 0.9 wt%). Since filter samples used for EDX analysis were sputtered with a layer of carbon, no information on the concentration of carbon could be obtained. Moreno et al. (2015) reported element concentrations for iron-rich particles of 40.0–65.0 wt% for Fe, 9.0–32.5 wt % for O, 2.0–19.5 wt% for C, and 1.0–8.5 wt% for Si. While our findings are in agreement with their Fe and O ranges, the amounts of Si vary, which might be explained by the usage of different steel types for train

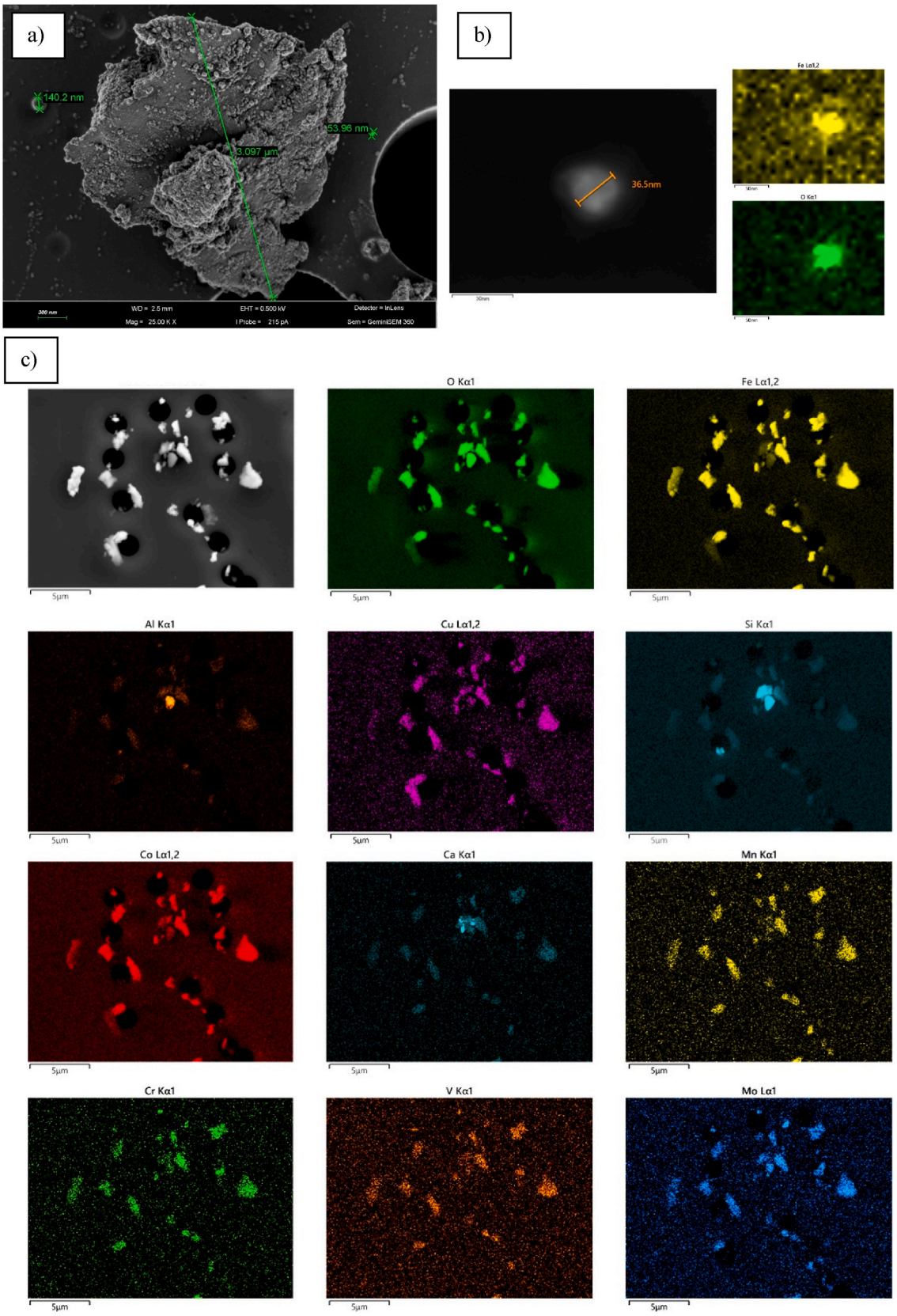

Fig. 5. a) SEM-micrograph of flake-like subway particle consisting predominantly of Fe and O with attached clusters of 20–30 nm sized spherical iron oxide and carbon containing particles, b) EDX mapping of 37 nm subway particle at 5 kV, c) EDX mapping of subway particles on a polycarbonate filter at 20 kV (size range of particles 200 nm–2.5 µm) Print in color.

rails and wheels in the Barcelona subway system, as well as differences in the composition of front and lateral brake pads between Munich and Barcelona.

Automated classification of EDX data showed that 75.43% of the >180 000 analyzed particles were made of iron oxides, while 5.35% consisted of metallic Fe and 1.23% belonged to geological, soil-derived particles. A total of 16.89% of all particles was not classified, however, large peaks for carbon and oxygen were observed in the spectra of these particles. This led to the assumption that these particles were mainly carbonaceous. Byeon et al. (2015) who used passive sampling reported values of 66 ± 9% for $PM_{2.5\text{-}1}$ in the Seoul subway system, while Jung et al. (2010) stated that 71 - 79% of all particles at stations without platform protection doors in Seoul consisted of iron-rich particles. These values are in accordance with our data highlighting the similarities in sampled subway aerosols around the globe.

The elemental distribution of Munich subway aerosol was similar for iron-rich particles of all analyzed sizes (250 nm - 5 μm) suggesting that the particles are originating from the same source. However, we observed that with decreasing particle size the ratio of iron to oxygen also decreased from Fe/O = 2.19 for particles of 5 μm to a ratio of Fe/O = 1.37 for particles of 250 nm. This can be explained by the increased ratio of surface area to volume of smaller particles, which facilitates oxidation processes at the surface of the particles.

Furthermore, clusters of nanoparticles adhering to larger ferruginous particles could be observed (Fig. 5), which were either iron-rich or of carbonaceous nature, and were also described by other research groups (Kang et al., 2008; Jung et al., 2010, 2012; Moreno et al., 2015). Iron oxide bearing nanoparticles were also found in an isolated form with their size ranging from 20 to 150 nm. An exemplary EDX mapping of a 37 nm iron oxide particle is given in Fig. 5b. Spherical Fe particles could originate from condensation of gaseous iron formed from sparking (Kang et al., 2008; Jung et al., 2010) while carbonaceous nanoparticles could be formed from oxidation of volatile organic compounds on the active metal surface of host particles (Kang et al., 2008; Moreno et al., 2015) or adhesion of soot particles from the outside air (Moreno et al., 2015; Grana et al., 2017). Graphite can also be found in brake pads and carbon particles can originate from electromotor brushes as discussed in Section 3.3. Literature suggests that iron oxides in the subway environment are present as hematite (Fe_2O_3), magnetite (Fe_3O_4) and maghemite (γ-Fe_2O_3) (Jung et al., 2012; Lu et al., 2015; Moreno et al., 2015), which we were not able to distinguish via EDX measurements.

Apart from the main elements Fe, O, and C the majority of particles in the subway aerosol was accompanied by trace elements such as Cu, Co, Mn, Cr, V, and Mo. These elements were also discovered by research groups world-wide (Kang et al., 2008; Jung et al., 2010; Midander et al., 2012; Moreno et al., 2015). Particles containing $BaSO_4$ or Sb that are attributed to brake wear and which were previously found in different subway systems (Kang et al., 2008; Moreno et al., 2015; Chang et al., 2021; Guseva Canu et al., 2021) were rare in the samples. In total, only 25 of >180 000 particles could be related to braking events via these metals. Fig. 5c shows an elemental mapping of subway particles on a PC filter.

While Munich subway aerosol (line *U5*) is similar in composition to subway systems in other cities, the often-reported Cu-rich particles, which are believed to originate from sparking and abrasion processes at the pantograph-catenary interface (Mugica-Álvarez et al., 2012; Moreno et al., 2015; Wang et al., 2016; Guseva Canu et al., 2021), were only scarcely observed in this study. In fact, only 220 of the total 182 020 particles analyzed were classified as Cu-rich and the reason might be that subway trains in Munich are powered by the third rail, which is made of low-carbon stainless steel at the sampled location (*https://www.u-bahn-muenchen.de/*).

Apart from iron-rich PM, several particles of supposedly geological origin were present in the samples. Particles attributed to this class consisted mainly of aluminium-magnesium silicates and quartz with occasional calcium carbonates, which is also described in the literature (Kang et al., 2008; Mugica-Álvarez et al., 2012; Byeon et al., 2015; Moreno et al., 2015; Perrino et al., 2015). These particles, as well as soot particles that were found in the samples, might entered the subway system by commuters or by mixing of in the subway generated aerosol with air from outside the system via ventilation (Kang et al., 2008; Mugica-Álvarez et al., 2012).

During the manual SEM-EDX analysis, we found several Fe-rich particles with layered structures interconnected by grooves. The structure and genesis of this particle type is unknown and has not been discussed in literature to our knowledge. A SEM micrograph and EDX spectra of one of the unknown particles, which consisted mainly of Fe, O, and C but also traces of Mn and Cr is given in Fig. S12 in the SI. The concentrations of Mn and Cr might indicate that the particle originated from some type of steel, however, its texture is not common for abrasion or evaporation derived particles but resembles more a crystalline structure. An additional EDX mapping of the particle class is given in Fig. S13 in the SI.

3.7. Summary

In the selected part of the *U-Bahn* subway line *U5*, PM_{10}, $PM_{2.5}$ and PM_1 concentrations at platforms ranged from 59 to 220, 27–80 and 9–21 μg m^{-3}, respectively. During typical trips, the average values ranged from 73 to 170, 29–59, 8 - 19 μg m^{-3}, respectively. The highest PM_{10} levels on the *CS-U2* platform were 231 ± 52 μg m^{-3}. Compared to WHO air quality recommendations, PM levels were generally high for long-term or repeated exposure, and mitigation measures for PM should be of great interest. The measured hot-spots could be classified as *very poor/extremely poor* compared to other subway systems (Cartenì et al., 2020). Most of the particle mass consisted of ferrous particles (FePM) from wheel and rail abrasion. Inadequate ventilation of platforms and tunnels is likely to be the cause of high PM levels. Probably for the same reason, subway PNC levels were not elevated even in the city center (10^3 - 10^4 pt cm^{-3}). Only a few cases of outdoor traffic-related particles with high PNC entering the subway platform were observed so ambient air was not the dominant source of PM.

Using mobile measurements, we observed a high spatial variability of PM among platforms and tunnel sections, which increased from the above-ground terminus *NS-U/S* towards downtown. The highest concentrations were measured at transfer stations with an overall high train frequency. The intra-day variability was mainly influenced by train frequency, so that PM concentrations were highest during the morning and afternoon rush-hour. Otherwise, concentrations at specific platforms were relatively stable over time (day of week, season). The same trend was observed from the eBC readings, but it is likely to be due to light-absorbing metal artifacts so further investigation of BC is needed.

The design of the station affected the concentrations – platforms with larger volumes tended to have lower PM concentrations than smaller with the same train frequency but the PM_{10} variability between these platforms was higher than on the double-track platforms. PM dynamics inside the train were high during rides due to the high air exchange with the outside tunnel. Old trains without air conditioning and with opened windows had slightly higher PM concentrations than new trains with air conditioning but the difference was less than 12% indicating poor or no filtration.

ICP-MS analysis quantified elevated levels of metals in the subway, particularly iron and metals present in the steel of the rails and wheels. Ferrous particles formed the majority of the aerosol mass. SEM-EDX analysis revealed the shape and size distribution of the metal particles. Trace elements typical for subways have been detected. The copper content in the Munich subway appeared to be lower than in other cities probably due to the absence of copper catenaries. Our results show that iron-rich particles and other metals are present even in the inhalable fraction of the aerosol, which could cause negative health effects. One of the described toxicological effects is the formation of reactive oxidative species (ROS) through the Fenton reaction, which can induce oxidative

stress (Kanti Das et al., 2014). However, most of the mass of these particles is formed by larger particles and not UFP, which can be deduced from the fact that PNC and LDSA in metro stations are not significantly elevated compared to ambient air values. Nevertheless, iron oxides nanoparticles around 30 nm were found. Given the potential association between iron nanoparticles and neurodegenerative diseases via the olfactory nerve entry route (Hopkins et al., 2018; Liu et al., 2018), toxicological investigations with real subway aerosol on this topic would be of interest.

To effectively mitigate air pollution, individual comprehensive measurements need to be made as subway systems can vary widely. While platform screen doors (PSD), air conditioning and other measures can reduce PM concentrations in the subway, they usually do not mitigate them completely (Chang et al., 2021; van Ryswyk et al., 2021). Measurements at selected platforms, as presented in other studies (Johansson and Johansson, 2003; Colombi et al., 2013; Moreno et al., 2014; Cusack et al., 2015; Chang et al., 2021), provide a comprehensive characterization of PM variability at one or several sites but often do not account for spatio-temporal variability in the wide variety of micro-environments during typical commuter rides. In addition, such campaigns can have high requirements on organization and equipment installation, which may be one reason why only a limited number of metro systems around the world have been characterized.

Based on our results, we propose to improve the air conditioning system of the new trains (ideally equipped with HEPA filters) and improve the ventilation of the platforms, but in such a way that there are no subway exhausts near busy streets or other sources of aerosol. More frequent dusting of the tracks and the best available brake system technology could also be beneficial. Wearing face-masks in subway could help to decrease the personal exposure from coarse particles as suggested by Ji et al. (2021), however, protection from nanoparticles is limited. Drivers and subway operators might be the most exposed to PM concentrations, so we propose to install air purifiers in the driver's cab.

The presented methodology for comprehensive air quality characterization in subways using a mobile measurement system has proven to be a fast and thorough way to determine the aerosol composition to which a subway passenger is exposed to. It can be used to map PM and PNC concentrations in different cities in a comparable manner by taking into account the high spatio-temporal variability of PM. Furthermore, realistic doses of specific pollutants can be calculated. This relatively low-cost approach typically requires no special preparations and measurements can be made rather effectively. Repeated trips can identify hot-spots and estimate personal exposure. Sampling for chemical analysis and particle imaging can reveal sources and potential health risks. In the future, it can be used to monitor potential air quality limits and the effectiveness of measures. The same system can also be used to compare different modes of transportation. Moreover, gas phase measurements and bioaerosol sampling can be added.

Funding sources

This research is funded by dtec.bw – Digitalization and Technology Research Center of the Bundeswehr [project LUKAS and MORE]. Dtec.bw is funded by the European Union – NextGenerationEU. This research was also supported by the project ULTRHAS – ULtrafine particles from TRansportation – Health Assessment of Sources, a project funded under the EU's Research and Innovation programme Horizon 2020, Grant Agreement No. 955390. We acknowledge financial support by Universität der Bundeswehr München.

CRediT authorship contribution statement

Jan Bendl: Conceptualization, Data curation, Formal analysis, Investigation, Methodology, Supervision, Visualization, Writing – original draft. **Carsten Neukirchen:** Formal analysis, Investigation, Methodology, Writing – original draft, Writing – review & editing. **Ajit Mudan:** Investigation. **Sara Padoan:** Investigation, Methodology, Writing – original draft. **Ralf Zimmermann:** Writing – review & editing. **Thomas Adam:** Conceptualization, Funding acquisition, Investigation, Methodology, Project administration, Resources, Supervision, Writing – review & editing.

Declaration of competing interest

The authors declare that they have no known competing financial interests or personal relationships that could have appeared to influence the work reported in this paper.

Data availability

Data will be made available on request.

Acknowledgement

Measurements were supported by students from the University of the Bundeswehr Munich M.Eng course Computer Aided Engineering (CAE): Ferdinand Lindenpütz, Moritz Tenckhoff, Rene Pfeiffer, Gregor Franke, Erik Milde. Construction of the measuring system was supported by the CAE master student Sören Möhrs.

Abbreviations

CPC	condensation particle counter
eBC	Equivalent Black Carbon
EC	Elemental Carbon
EDX	energy-dispersive X-ray spectroscopy
GPS	Global positioning system
ICP-MS	Inductively coupled plasma mass spectrometry
LDSA	lung deposited surface area
NEE	non-exhaust emissions
OC	Organic Carbon
ONA	Optimized Noise-Reduction Averaging
OPS	Optical particle sizer
PC	Polycarbonate
PAHs	Polycyclic Aromatic Hydrocarbons
PM	Particulate Matter
PM_x	particulate matter smaller than X μm in the aerodynamic diameter
PNC	particle number concentration
PSD	platform screed doors
SEM-EDX	Scanning electron microscopy with energy dispersive X-ray spectroscopy
SIA	secondary inorganic aerosols
UFP	ultrafine particles
UVPM	ultraviolet absorbing particulate matter

Appendix A. Supplementary data

Supplementary data to this article can be found online at https://doi.org/10.1016/j.atmosenv.2023.119883.

References

Aarnio, P., Yli-Tuomi, T., Kousa, A., Mäkelä, T., Hirsikko, A., Hämeri, K., Räisänen, M., Hillamo, R., Koskentalo, T., Jantunen, M., 2005. The concentrations and composition of and exposure to fine particles (PM2.5) in the Helsinki subway system. Atmos. Environ. 39, 5059–5066.

Bachoual, R., Boczkowski, J., Goven, D., Amara, N., Tabet, L., On, D., Leçon-Malas, V., Aubier, M., Lanone, S., 2007. Biological effects of particles from the paris subway system. Chem. Res. Toxicol. 20, 1426–1433.

Braniš, M., 2006. The contribution of ambient sources to particulate pollution in spaces and trains of the Prague underground transport system. Atmos. Environ. 40, 348–356.

Byeon, S.-H., Willis, R., Peters, T.M., 2015. Chemical characterization of outdoor and subway fine (PM(2.5-1.0)) and coarse (PM(10-2.5)) particulate matter in Seoul (Korea) by computer-controlled scanning electron microscopy (CCSEM). Int. J. Environ. Res. Publ. Health 12, 2090–2104.
Cartenì, A., Cascetta, F., Campana, S., 2015. Underground and ground-level particulate matter concentrations in an Italian metro system. Atmos. Environ. 101, 328–337.
Cartenì, A., Cascetta, F., Henke, I., Molitierno, C., 2020. The role of particle resuspension within PM concentrations in underground subway systems. Int. J. Environ. Sci. Technol. 17, 4075–4094.
Cepeda, M., Schoufour, J., Freak-Poli, R., Koolhaas, C.M., Dhana, K., Bramer, W.M., Franco, O.H., 2017. Levels of ambient air pollution according to mode of transport: a systematic review. Lancet Public Health 2, e23–e34.
Cha, Y., Olofsson, U., 2018. Effective density of airborne particles in a railway tunnel from field measurements of mobility and aerodynamic size distributions. Aerosol. Sci. Technol. 52, 886–899.
Chang, L., Chong, W.T., Wang, X., Pei, F., Zhang, X., Wang, T., Wang, C., Pan, S., 2021. Recent progress in research on PM2.5 in subways. Environmental science. Processes & impacts 23, 642–663.
Colombi, C., Angius, S., Gianelle, V., Lazzarini, M., 2013. Particulate matter concentrations, physical characteristics and elemental composition in the Milan underground transport system. Atmos. Environ. 70, 166–178.
Cusack, M., Talbot, N., Ondráček, J., Minguillón, M.C., Martins, V., Klouda, K., Schwarz, J., Ždímal, V., 2015. Variability of aerosols and chemical composition of PM 10 , PM 2.5 and PM 1 on a platform of the Prague underground metro. Atmos. Environ. 118, 176–183.
Font, O., Moreno, T., Querol, X., Martins, V., Sánchez Rodas, D., Miguel, E. de, Capdevila, M., 2019. Origin and speciation of major and trace PM elements in the Barcelona subway system. Transport. Res. Transport Environ. 72, 17–35.
Grana, M., Toschi, N., Vicentini, L., Pietroiusti, A., Magrini, A., 2017. Exposure to ultrafine particles in different transport modes in the city of Rome. Environmental pollution (Barking, Essex : 1987 228, 201–210.
Guseva Canu, I., Crézé, C., Hemmendinger, M., Ben Rayana, T., Besançon, S., Jouannique, V., Debatisse, A., Wild, P., Sauvain, J.J., Suárez, G., Hopf, N.B., 2021. Particle and metal exposure in Parisian subway: relationship between exposure biomarkers in air, exhaled breath condensate, and urine. Int. J. Hyg Environ. Health 237, 113837.
Hagler, G.S., Yelverton, T.L., Vedantham, R., Hansen, A.D., Turner, J.R., 2011. Post-processing method to reduce noise while preserving high time resolution in aethalometer real-time black carbon data. Aerosol Air Qual. Res. 11, 539–546.
Hopkins, L.E., Laing, E.A., Peake, J.L., Uyeminami, D., Mack, S.M., Li, X., Smiley-Jewell, S., Pinkerton, K.E., 2018. Repeated iron-soot exposure and nose-to-brain transport of inhaled ultrafine particles. Toxicol. Pathol. 46, 75–84.
Huck, W. (Ed.), 2022. Sustainable Development Goals. Nomos Verlagsgesellschaft mbH & Co. KG.
Ji, W., Li, X., Wang, C., 2021. Composition and exposure characteristics of PM2.5 on subway platforms and estimates of exposure reduction by protective masks. Environ. Res. 197, 111042.
Ji, W., Zhao, K., Liu, C., Li, X., 2022. Spatial characteristics of fine particulate matter in subway stations: source apportionment and health risks. Environmental pollution (Barking, Essex : 1987 305, 119279.
Johansson, C., Johansson, P.-Å., 2003. Particulate matter in the underground of Stockholm. Atmos. Environ. 37, 3–9.
Jung, H.-J., Kim, B., Malek, M.A., Koo, Y.S., Jung, J.H., Son, Y.-S., Kim, J.-C., Kim, H., Ro, C.-U., 2012. Chemical speciation of size-segregated floor dusts and airborne magnetic particles collected at underground subway stations in Seoul, Korea. J. Hazard Mater. 213–214, 331–340.
Jung, H.-J., Kim, B., Ryu, J., Maskey, S., Kim, J.-C., Sohn, J., Ro, C.-U., 2010. Source identification of particulate matter collected at underground subway stations in Seoul, Korea using quantitative single-particle analysis. Atmos. Environ. 44, 2287–2293.
Kang, S., Hwang, H., Park, Y., Kim, H., Ro, C.-U., 2008. Chemical compositions of subway particles in Seoul, Korea determined by a quantitative single particle analysis. Environ. Sci. Technol. 42, 9051–9057.
Kanti Das, T., Wati, M.R., Fatima-Shad, K., 2014. Oxidative stress gated by Fenton and haber weiss reactions and its association with alzheimer's disease. Arch Neurosci 2.
Karlsson, H.L., Holgersson, A., Möller, L., 2008. Mechanisms related to the genotoxicity of particles in the subway and from other sources. Chem. Res. Toxicol. 21, 726–731.
Karlsson, H.L., Ljungman, A.G., Lindbom, J., Möller, L., 2006. Comparison of genotoxic and inflammatory effects of particles generated by wood combustion, a road simulator and collected from street and subway. Toxicol. Lett. 165, 203–211.
Licina, D., Tian, Y., Nazaroff, W.W., 2017. Emission rates and the personal cloud effect associated with particle release from the perihuman environment. Indoor Air 27, 791–802.
Liu, J.-L., Fan, Y.-G., Yang, Z.-S., Wang, Z.-Y., Guo, C., 2018. Iron and alzheimer's disease: from pathogenesis to therapeutic implications. Front. Neurosci. 12, 632.
Liu, X., Hadiatullah, H., Zhang, X., Hill, L.D., White, A.H.A., Schnelle-Kreis, J., Bendl, J., Jakobi, G., Schloter-Hai, B., Zimmermann, R., 2021. Analysis of Mobile Monitoring Data from the microAeth® MA200 for Measuring Changes in Black Carbon on the Roadside in Augsburg, p. 13.
Loxham, M., Cooper, M.J., Gerlofs-Nijland, M.E., Cassee, F.R., Davies, D.E., Palmer, M.R., Teagle, D.A.H., 2013. Physicochemical characterization of airborne particulate matter at a mainline underground railway station. Environ. Sci. Technol. 47, 3614–3622.
Lu, S., Liu, D., Zhang, W., Liu, P., Fei, Y., Gu, Y., Wu, M., Yu, S., Yonemochi, S., Wang, X., Wang, Q., 2015. Physico-chemical characterization of PM2.5 in the microenvironment of Shanghai subway. Atmos. Res. 153, 543–552.
Lyu, Y., Olofsson, U., 2020. On black carbon emission from automotive disc brakes. J. Aerosol Sci. 148, 105610.
Martins, V., Cruz Minguillón, M., Moreno, T., Querol, X., Miguel, E. de, Capdevila, M., Centelles, S., Lazaridis, M., 2015. Deposition of aerosol particles from a subway microenvironment in the human respiratory tract. J. Aerosol Sci. 90, 103–113.
Martins, V., Moreno, T., Mendes, L., Eleftheriadis, K., Diapouli, E., Alves, C.A., Duarte, M., Miguel, E. de, Capdevila, M., Querol, X., Minguillón, M.C., 2016. Factors controlling air quality in different European subway systems. Environ. Res. 146, 35–46.
Midander, K., Elihn, K., Wallén, A., Belova, L., Karlsson, A.-K.B., Wallinder, I.O., 2012. Characterisation of nano- and micron-sized airborne and collected subway particles, a multi-analytical approach. Sci. Total Environ. 427–428, 390–400.
Minguillón, M.C., Reche, C., Martins, V., Amato, F., Miguel, E. de, Capdevila, M., Centelles, S., Querol, X., Moreno, T., 2018. Aerosol sources in subway environments. Environ. Res. 167, 314–328.
Moreno, T., Martins, V., Querol, X., Jones, T., BéruBé, K., Minguillón, M.C., Amato, F., Capdevila, M., Miguel, E. de, Centelles, S., Gibbons, W., 2015. A new look at inhalable metalliferous airborne particles on rail subway platforms. Sci. Total Environ. 505, 367–375.
Moreno, T., Pérez, N., Reche, C., Martins, V., Miguel, E. de, Capdevila, M., Centelles, S., Minguillón, M.C., Amato, F., Alastuey, A., Querol, X., Gibbons, W., 2014. Subway platform air quality: assessing the influences of tunnel ventilation, train piston effect and station design. Atmos. Environ. 92, 461–468.
Mugica-Álvarez, V., Figueroa-Lara, J., Romero-Romo, M., Sepúlveda-Sánchez, J., López-Moreno, T., 2012. Concentrations and properties of airborne particles in the Mexico City subway system. Atmos. Environ. 49, 284–293.
Perrino, C., Marcovecchio, F., Tofful, L., Canepari, S., 2015. Particulate matter concentration and chemical composition in the metro system of Rome, Italy. Environ. Sci. Pollut. Res. 22, 9204–9214.
Querol, X., Moreno, T., Karanasiou, A., Reche, C., Alastuey, A., Viana, M., Font, O., Gil, J., Miguel, E., de, Capdevila, M., 2012. Variability of levels and composition of PM_{10} and $PM_{2.5}$ in the Barcelona metro system. Atmos. Chem. Phys. 12, 5055–5076.
Roy, D., Lyou, E.S., Kim, J., Lee, T.K., Park, J., 2022. Commuters health risk associated with particulate matter exposures in subway system – globally. Build. Environ. 216, 109036.
Rupprecht Consult, 2019. Guidelines for Developing and Implementing a Sustainable Urban Mobility Plan, second ed., p. 168
Salo, L., Rönkkö, T., Saarikoski, S., Teinilä, K., Kuula, J., Alanen, J., Arffman, A., Timonen, H., Keskinen, J., 2021. Concentrations and size distributions of particle lung-deposited surface area (LDSA) in an underground mine. Aerosol Air Qual. Res. 21, 200660.
Schraufnagel, D.E., 2020. The health effects of ultrafine particles. Exp. Mol. Med. 52, 311–317.
Shakya, K.M., Saad, A., Aharonian, A., 2020. Commuter exposure to particulate matter at underground subway stations in Philadelphia. Build. Environ. 186, 107322.
Targino, A.C., Krecl, P., Brimblecombe, P., Oukawa, G.Y., Danziger Filho, J.E., Moreno, F.L., 2021. Spatio-temporal variability of airborne particulate matter in the São Paulo subway. Build. Environ. 189, 107526.
van Ryswyk, K., Anastasopolos, A.T., Evans, G., Sun, L., Sabaliauskas, K., Kulka, R., Wallace, L., Weichenthal, S., 2017. Metro commuter exposures to particulate air pollution and PM2.5-associated elements in three Canadian cities: the urban transportation exposure study. Environ. Sci. Technol. 51, 5713–5720.
van Ryswyk, K., Kulka, R., Marro, L., Yang, D., Toma, E., Mehta, L., McNeil-Taboika, L., Evans, G.J., 2021. Impacts of Subway System Modifications on Air Quality in Subway Platforms and Trains. Environmental science & technology. https://doi.org/10.1021/acs.est.1c00703.
Wang, B.-Q., Liu, J.-F., Ren, Z.-H., Chen, R.-H., 2016. Concentrations, properties, and health risk of PM2.5 in the Tianjin City subway system. Environ. Sci. Pollut. Res. Int. 23, 22647–22657.
World Health Organization, 2021. WHO Global Air Quality Guidelines: Particulate Matter (PM2.5 and PM10), Ozone, Nitrogen Dioxide, Sulfur Dioxide and Carbon Monoxide. WHO European Centre for Environment and Health, Bonn, Germany, p. 285.
Xu, B., Hao, J., 2017. Air quality inside subway metro indoor environment worldwide: a review. Environ. Int. 107, 33–46.
Xu, B., Yu, X., Gu, H., Miao, B., Wang, M., Huang, H., 2016. Commuters' exposure to PM2.5 and CO2 in metro carriages of Shanghai metro system. Transport. Res. Transport Environ. 47, 162–170.
Yang, F., Kaul, D., Wong, K.C., Westerdahl, D., Sun, L., Ho, K., Tian, L., Brimblecombe, P., Ning, Z., 2015. Heterogeneity of passenger exposure to air pollutants in public transport microenvironments. Atmos. Environ. 109, 42–51.
Zhao, L., Wang, J., Gao, H.O., Xie, Y., Jiang, R., Hu, Q., Sun, Y., 2017. Evaluation of particulate matter concentration in Shanghai's metro system and strategy for improvement. Transport. Res. Transport Environ. 53, 115–127.